Supplementary Information

A Two-Dimensional Zeolitic Imidazolate Framework with a Cushion-Shaped Cavity for CO_2 Adsorption

Rizhi Chen, [a,b] *Jianfeng Yao,* [a] *Qinfen Gu,* [c] *Stef Smeets,* [d] *Christian Baerlocher,* [d] *Haoxue Gu,* [b] *Dunru Zhu,* [b] *William Morris,* [e] *Omar M. Yaghi,* [f] *Huanting Wang*[*a]

[a] *Department of Chemical Engineering, Monash University, Clayton, Victoria 3800, Australia. Email: huanting.wang@monash.edu*

[b] *State Key Laboratory of Materials-Oriented Chemical Engineering, Nanjing University of Technology, Nanjing 210009, P. R. China*

[c] *Australian Synchrotron, Clayton, Vic 3168, Australia*

[d] *ETH Zurich, Laboratory of Crystallography, CH-8093 Zurich, Switzerland*

[e] *Department of Chemistry, Northwestern University, Evanston, IL 60208, USA*

[f] *Department of Chemistry, University of California-Berkeley, and Molecular Foundry, Lawrence Berkeley National Laboratory, Berkeley, CA 94720, USA*

Sample synthesis and characterization

$Zn(NO_3)_2 \cdot 6H_2O$ (98%) and 2-methylimidazole (Hmim) (99%) were purchased from Sigma-Aldrich, and used as received without further purification. ZIF-L crystals with leaf-like morphology were synthesized at room temperature in an aqueous system with a Hmim to zinc ions molar ratio of 8. Typically, 0.59 g of $Zn(NO_3)_2 \cdot 6H_2O$ and 1.30 g of Hmim were dissolved in 40 mL deionized water respectively, and then the aqueous solution of zinc nitrate was added into the aqueous solution of Hmim under stirring. The mixture was stirred at room temperature for 4 h. The product was collected by repeated centrifugation (at 6000 rpm for 20 min) and washed by water for three times, and then dried in an oven at 70 ˚C overnight.

SEM images were taken with a JSM-7100F microscope (JEOL). Nitrogen physisorption isotherms were measured at 77 K on an automatic volumetric adsorption apparatus (Micromertics ASAP

2020). CO_2 and CH_4 adsorption isotherms were obtained with a Micromeritics ASAP 2010 analyzer at room temperature. The samples were activated in hot methanol (60 ^oC). After drying, they were degassed at 383 K for 24 h prior to the sorption measurements. Elemental analysis of as-prepared ZIF-L was performed by the Galbraith Laboratories, Inc. Knoxville, TN 37921-1750, USA

Elemental composition of as-synthesized ZIF-L

The composition of ZIF-L prior to activation was determined to be $Zn(mim)_2 \cdot (Hmim)_{1/2} \cdot (H_2O)_{3/2}$ ($C_{10}H_{16}N_5O_{3/2}Zn$) from the elemental analysis result (C: 40.50; H: 4.86; N: 25.30). The values calculated from the above molecular formula: C: 40.62; H: 5.45; N: 23.69. This result was confirmed by the TGA analysis (Fig. S1).

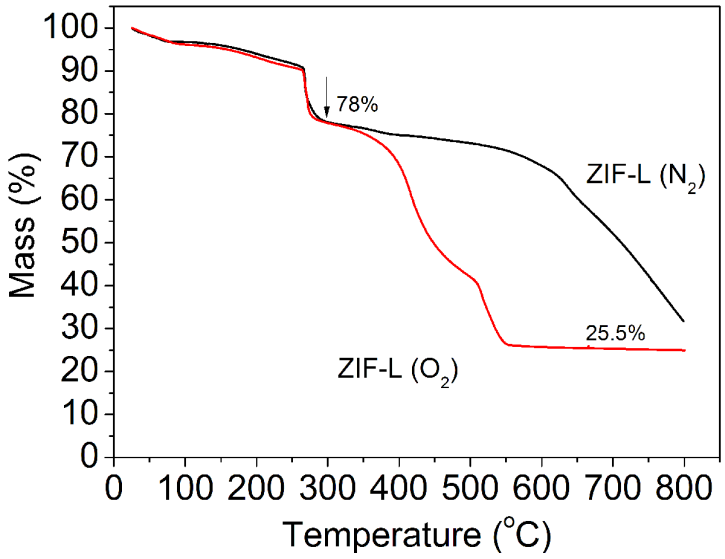

Fig. S1. TG curves of as-synthesized ZIF-L recorded under flowing oxygen and nitrogen. At 300 ^oC, the mass residue for both TG curves is about 78%, which agrees well with the mass loss arising from the removal of the weakly linked ½ Hmim and guest water molecule. For the TG curve under O_2, the mass residue at 700 ^oC is about 25.5%, indicating that ZIF-L is totally transferred into ZnO (The calculation was made on the basis of molecular masses of $Zn(mim)_2 \cdot (Hmim)_{1/2} \cdot (H_2O)_{3/2}$ (295) and ZnO (81)).

ZIF-L structural determination from Powder XRD

Synchrotron powder diffraction data for as-synthesized ZIF-L were collected with a wavelength of 0.8237 Å with a Mythen-II detector on the Powder diffraction beamline at the Australian Synchrotron with a step size of 0.00375˚ 2θ. As-synthesized sample was gently ground in a mortar,

and then loaded into 0.7 mm glass capillaries. The pattern was indexed with an orthorhombic unit cell (a = 24.0610 Å, b = 16.9673 Å, c = 19.6783 Å) using the program Topas.[1] The large background at low angles was manually removed and data was binned to 0.01˚ 2θ to eliminate the noise in the data. This significantly eased the extraction of the reflection intensities using the Pawley peak fitting procedure in Topas. The structure solution was started using the powder charge-flipping algorithm (pCF) implemented in the program Superflip.[2] Two Zn atoms were easily located in the electron density maps and the space group was determined to be *Cmce*. However, it was difficult to locate the imidazole molecules directly. The Zn-Zn framework distance of 6.0 Å was consistent with that of similar ZIF structures, so a tentative model could be constructed by placing Mim molecules midway between the Zn atoms. The correct orientation of the Mim molecules was found with the program Topas in the following way: Zn-Mim-Zn fragments were constructed as rigid bodies. The Zn atoms were treated as dummy atoms in the rigid body fragments and their positions were restrained to the positions located in the pCF electron density maps. Consequently, the orientation of the Mim fragments could be refined by allowing rotations only around their respective Zn-Zn axis. This essentially reduced the number of parameters for the orientation of the Mim molecules to 4. The starting orientations were randomised for many runs in order to eliminate the possibility of local minima and optimised considering intermolecular distance. Using difference Fourier maps a 5th Mim molecule could be located that connected to the "free" N46-atoms of two monodentate Mim-4 molecules. The N46 – N55 distance refined to 2.66 Å which is somewhat shorter than the N-H···N hydrogen bond distance of 2.82 Å found in the crystal structure of 2-methylimidazole.[3] Further improvements to the structure could be made by locating two water molecules in the voids using difference Fourier maps. Refinement of the framework converged with an R_{wp} value of 0.0755.

To get a better understanding of the CO_2 sorption the XRD data collected for the 100 kPa sorption experiment were used in a Rietveld refinement. Since the sorption of CO_2 did not change the XRD pattern significantly, the structure of the as made sample could be used as a starting point. All cell parameters were somewhat shorter after the sorption, resulting in a volume decrease of the unit cell of 1.15%. The CO_2 molecule could be located in the cavity using difference Fourier maps. It was refined to an occupancy of about 0.5, so it was fixed at this value. There are two symmetrically equivalent CO_2 molecules in the cavity with an O…O distance of 2.5 Å, which

means that both molecules are probably not present at the same time. An additional water position was also found in the cavity that was also fixed at an occupancy of 0.5. Apparently, the *in-situ* outgassing on the capillary was not complete. The total amount of CO_2 found in the refinement is about 1 mmol/g, which is in good agreement with the value found in the sorption experiment.

In both refinements the Hmim molecules were geometrically restricted to the bond distances found in the single crystal refinement of 2-Methylimidazole.[3] In addition, soft restraints were applied the Zn-N distances and N-Zn-N tetrahedral angles. Except for the Zn atoms, the displacement factors were constraint to be the same for each atom type. Details of the data collection and refinements are listed in Table S1.

***In-situ* XRD measurements**

High pressure synchrotron x-ray diffraction experiments were performed at the Powder diffraction beamline, Australian Synchrotron. The 2D diffraction data were collected on a Mar165 CCD detector using a wavelength of 0.6881 Å. The 2D diffraction images were integrated by the use of the program fit2d. High pressures up to 6.3 GPa were generated by use of a diamond anvil cell (easyLab) at room temperature. A mixture of methanol and ethanol (4:1) was served as pressure-transmitting medium. To minimize deviatoric stress, the amount of pressure medium covered ca. 30% of the total volume (materials 70%) of the sample chamber within a rhenium gasket. A ruby crystal was placed into the sample chamber as a pressure marker and the pressures were determined using the ruby fluorescence technique. For *in-situ* CO_2 absorption measurements, the sample was first loaded into a 0.7 mm quartz capillary into a flow cell, and then it was pumped under vacuum overnight at 100 °C. After cooling down to room temperature in vacuum the flow cell was mounted onto the diffractometer for XRD measurement, then high purity CO_2 (99.99%) was introduced into the flow cell and stabilized for 5 min with 10 min data collection time at 20, 50, and 100 kPa, respectively. The refined XRD results show that the H_2O molecules cannot be totally pumped out from the structure; this may due to insufficient vacuum from the roughing pump (about 10^{-3} torr).

Table S1. Experimental and crystallographic data for ZIF-L

	ZIF-L at 298K	ZIF-L CO_2 at 100kPa
Data Collection		
Synchrotron facility	Australian Synchrotron	
Beamline	Powder diffraction	
Wavelength (Å)	0.8237	0.6881
Detector	Mythen-II	Mythen-II
Unit Cell		
Space group	Cmce	Cmce
a	24.1191(5)	24.0175(5)
b	17.0604(3)	17.0004(4)
c	19.7398(4)	19.6651(4)
Refinement		
2θ range (˚2θ) used	3.0 - 40.0	2.7 - 40.0
step size (˚2θ)	0.01 (binned)	0.01 (binned)
Number of observations	3700	3699
Soft restrictions		96
Zn-N		1.985 Å
N-Zn-N		109.47˚
Number of rigid Mim's	5	
Number of structural parameters	75	91
R_{wp}	0.075	0.134
R_{exp}	0.049	0.124

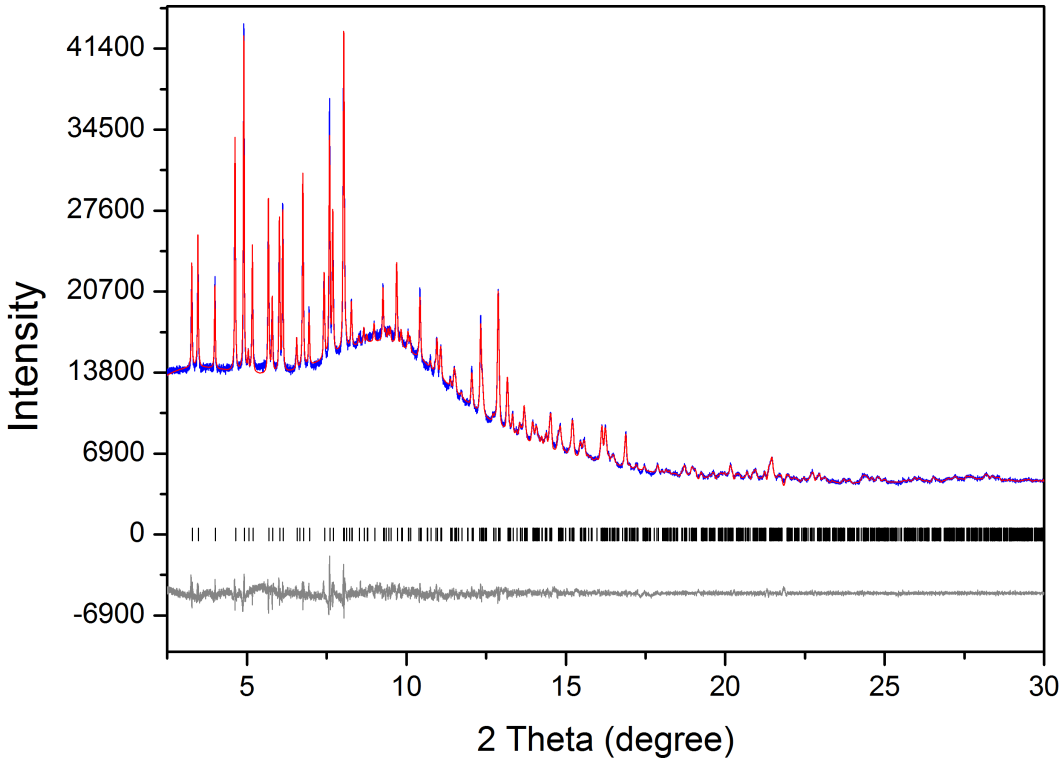

Fig. S2. Rietveld refinement profile for ZIF-L sample showing observed (blue line), calculated (red line), and difference (grey line) plots. The positions of Bragg reflections (tick marks) are shown for ZIF-L. The data was collected at a wavelength of 0.6881 Å at room temperature under 100 kPa CO_2.

Table S2. Comparison of CO_2 adsorption capacity for various ZIFs and MOFs.

Sample	Temperature /K	Pressure /MPa	CO_2 uptake /mmol/g	CO_2/CH_4 Selectivity	Reference
ZIF-L	298	0.1	0.94	7.2	this work
ZIF-8	298	0.1	0.66	2.8	this work
ZIF-100	298	0.1	0.9	4.1	[4]
ZIF-95	298	0.1	0.8	3.6	[4]
ZIF-8	298	0.1	0.45	-	[5]
ZIF-8	298	0.1	0.68	-	[6]
ZIF-8	298	0.1	0.78	2.8	[7]
ZIF-8	298	0.1	0.57	-	[8]
ZIF-8	298	0.1	0.60	2.6	[9]
ZIF-20	273	0.1	3.13	5	[10]
ZIF-25, -71, -93, 96,-97	298	0.1	0.6~2.1	-	[11]
MOF-177	298	0.1	1.36	2.3	[12]
MOF-5	298	0.1	0.91	7.2	[12]
MIL-53 (Cr)	304	2	8.6	2.0	[13]
MIL-53 (Al)	303	2	6.3	3.0	[14]
MIL-53 (Al)	304	2	9.8	2.04	[15]
MIL-53 (Cr)	304	2	9.5	1.9	[15]
MIL-101c (Cr)	303	5	40	3.1	[16]
Cu-BTC	303	4	14	1.53	[17]
MOF-508b	303	0.45	5.9	3.1	[18]
Cu-HBTB	298	2	5.6	1.75	[19]
NOTT-300	273	0.1	7.0	100	[20]
UIO-66	306	2	6.4	2.4	[21]

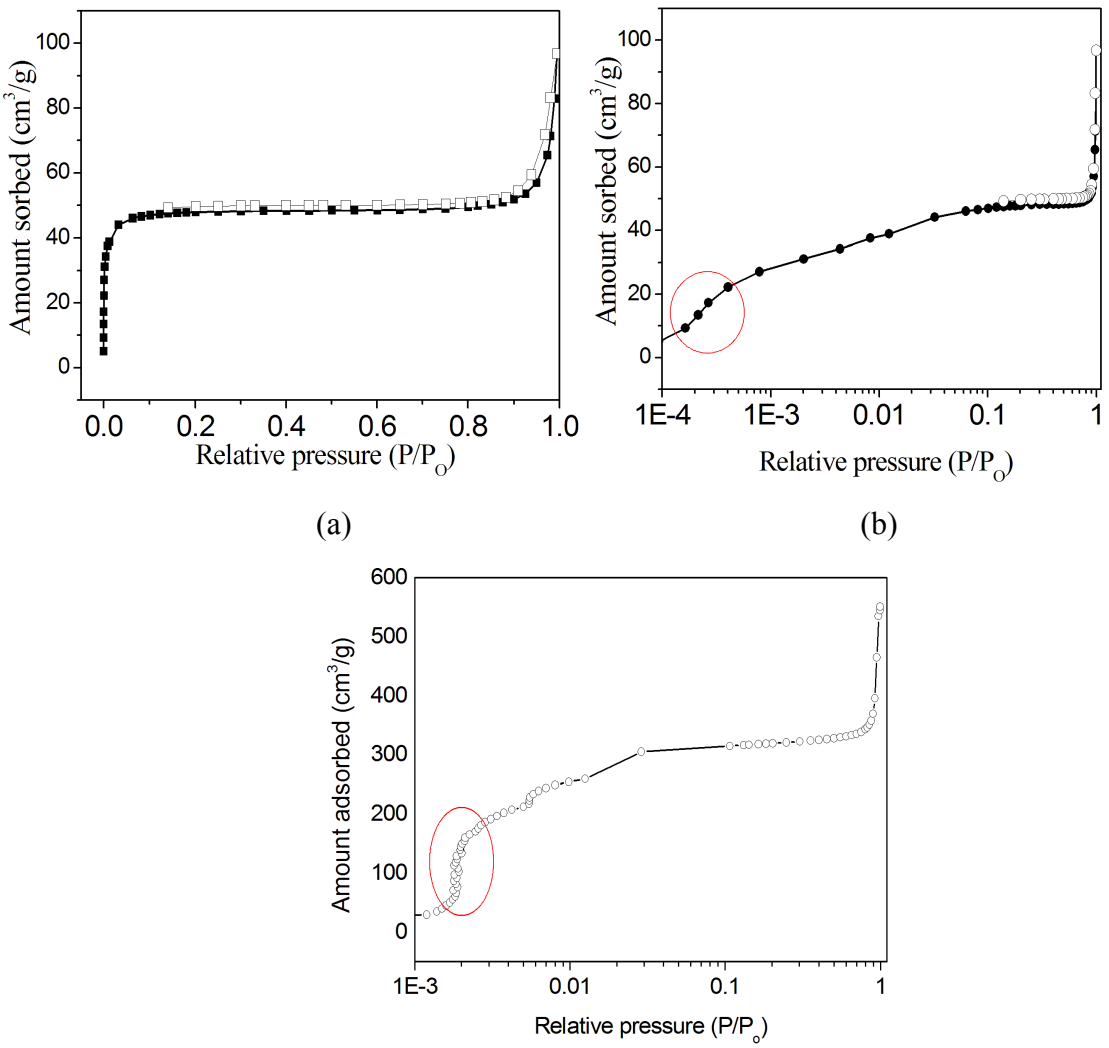

Fig. S3. (a) Nitrogen adsorption-desorption isotherm and (b) its semi-log plot for ZIF-L, and (c) semi-plot for N_2 adsorption isotherm of ZIF-8. The nitrogen sorption experiments were carried out at 77K. Fig.3c shows that there is a sharp increase in the amount of nitrogen adsorbed at low relative pressures (red-circled), indicating the gate-opening adsorption process. In contrast, the gate-opening adsorption also occurs in ZIF-L, but it is much less significant than that in ZIF-8.

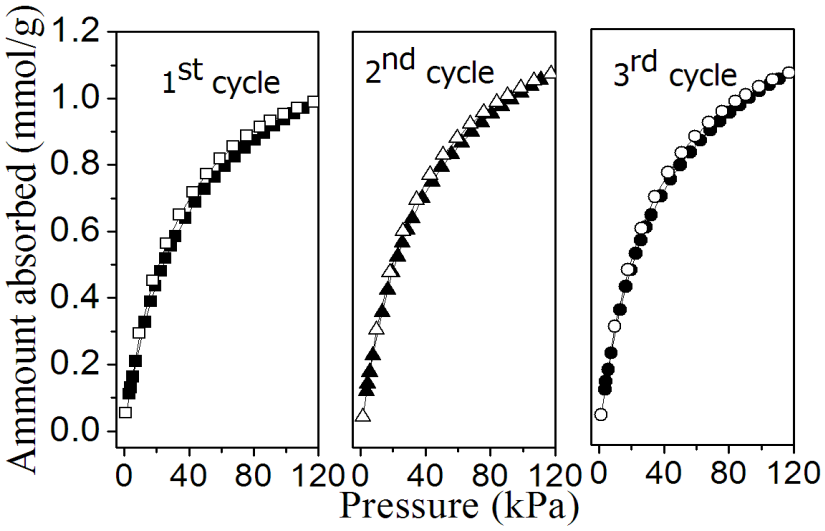

Fig. S4. CO_2 adsorption-desorption isotherms of ZIF-L at 1-3 cycles at 298 K.

Thermal stability of ZIF-L

The thermal stability of as-synthesized ZIF-L was investigated in open air at elevated temperature for 5 h. XRD patterns were recorded on a Philips PW1140/90 diffractometer with Cu Kα radiation (25 mA and 40 kV) at a scan rate of 2°/min with a step size of 0.01°. The sample treated at 150 ^{o}C almost had no changes in XRD pattern, color and morphology (Fig.s S5-S10). The leaf-shaped ZIF-L started to decompose at 200 ^{o}C and the color changed from white to dark yellow. The ZIF crystal structure was completely destroyed and oxidized into ZnO after being heated at 500 ^{o}C, and the color turned back to white (Fig. S6). For comparison, we also investigated its thermal stability in vacuum. ZIF-L retained its framework structure and the leaf-like morphology (Fig.s S7, and S10) even after 24 h of heating at 110 ^{o}C, indicating that the release of guest molecules (mainly water) does not affect the framework structure. As the sample was heated to 150 ^{o}C, the peak intensity of the XRD pattern decreased significantly, and the color changed to yellow and some of the leaf-like crystals broke into small particles. These results indicate that the stability of the ZIF-L is better in air than in vacuum.

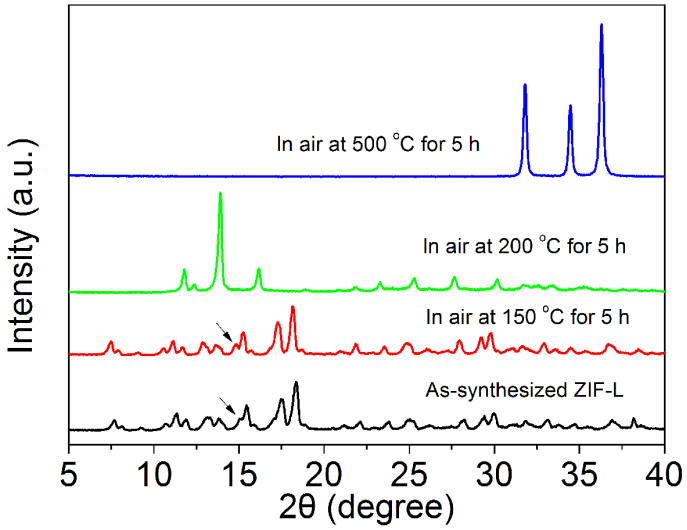

Fig. S5. XRD patterns of as-synthesized ZIF-L treated in air. For as-synthesized ZIF-L treated at 150 °C for 5 h, the intensity of XRD peak at around 15° changes, indicating the removal of the guest molecules (H_2O).

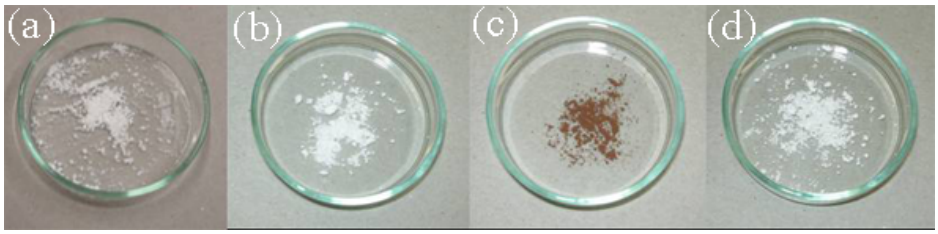

Fig. S6. Photographs of as-synthesized ZIF-L treated in air.

(a) as-synthesized, (b) 150 °C for 5 h, (c) 200 °C for 5 h, (d) 500 °C for 5 h.

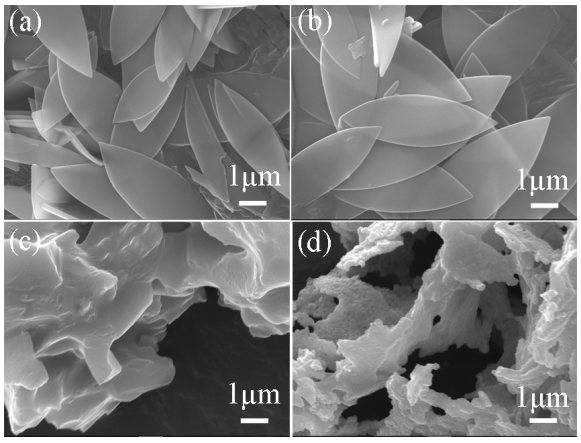

Fig. S7. SEM images of as-synthesized ZIF-L treated in air.

(a) as-synthesized, (b) 150 °C for 5 h, (c) 200 °C for 5 h, and (d) 500 °C for 5 h.

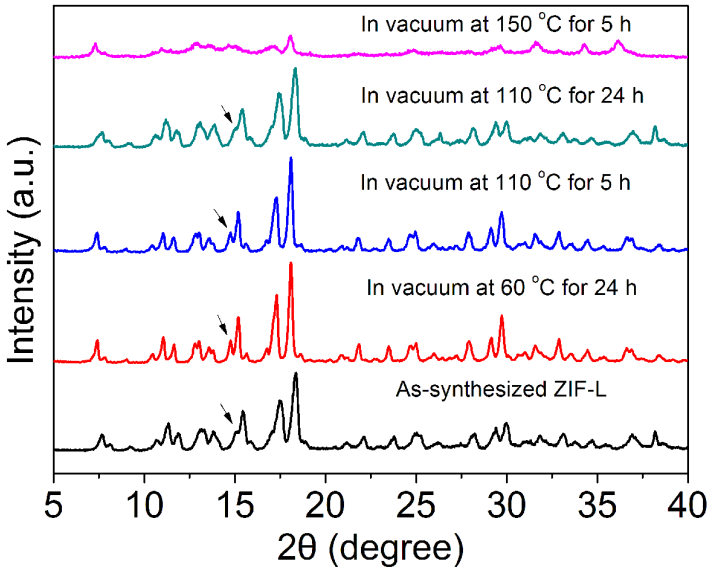

Fig. S8. XRD of as synthesized ZIF-L treated under vacuum. For as-synthesized ZIF-L treated in vacuum above 60 °C, the change of the intensity of XRD peak at around 15° indicates the removal of the guest molecules (H_2O).

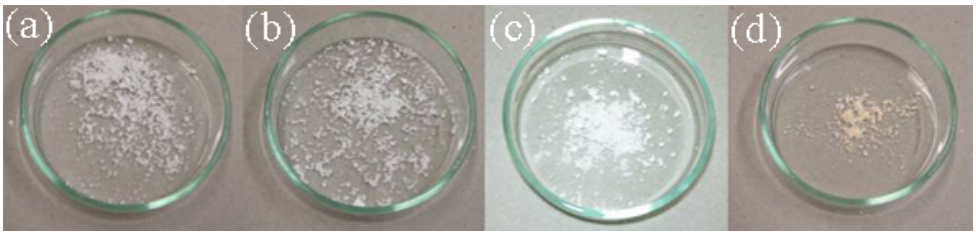

Fig. S9. Photographs of as synthesized ZIF-L treated under vacuum.

(a) 60 °C for 24 h, (b) 110 °C for 5 h, (c) 110 °C for 24h, and (d) 150 °C for 5 h

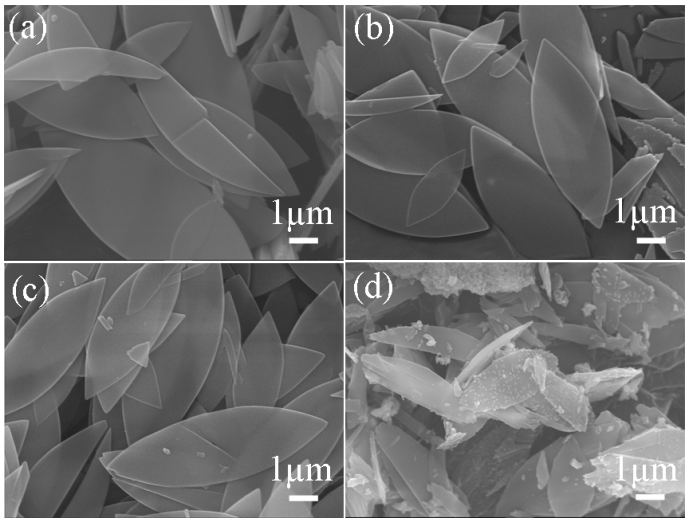

Fig. S10. FESEM of as synthesized ZIF-L treated under vacuum.

(a) 60 °C for 24 h, (b) 110 °C for 5 h, (c) 110 °C for 24h, and (d) 150 °C for 5 h.

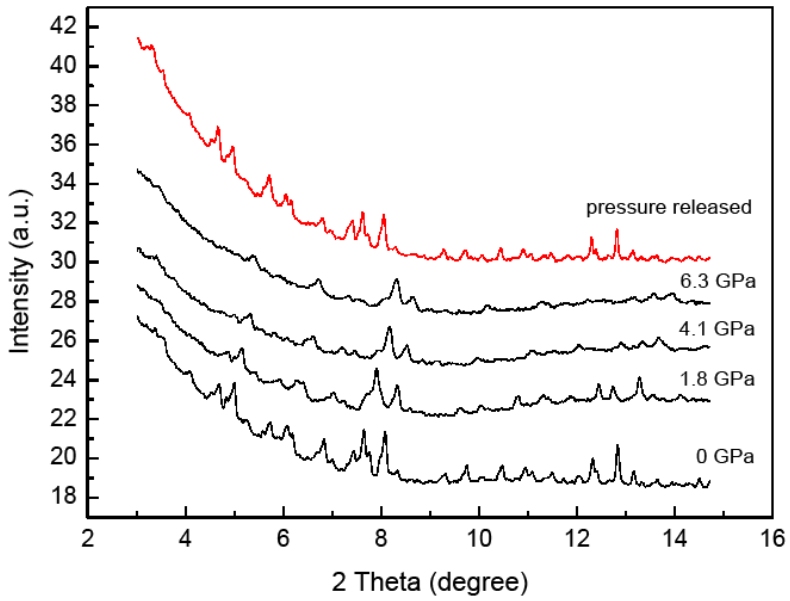

Fig. S11. X-ray powder diffraction patterns of ZIF-L at different pressures. The data was collected at a wavelength of 0.6881 Å at the powder diffraction beamline, Australian Synchrotron.

References

1. A. Coelho, 2007, http://www.topas-academic.net/.
2. L. Palatinus and G. Chapuis, *J. Appl. Crystallogr.*, 2007, **40**, 786-790.
3. B. Hachula, M. Nowak and J. Kusz, *J. Chem. Crystallogr.*, 2010, **40**, 201-206.
4. B. Wang, A. P. Cote, H. Furukawa, M. O'Keeffe and O. M. Yaghi, *Nature*, 2008, **453**, 207-U206.

5. S. K. Nune, P. K. Thallapally, A. Dohnalkova, C. M. Wang, J. Liu and G. J. Exarhos, *Chem. Commun.*, 2010, **46**, 4878-4880.
6. C. Chen, J. Kim, D. A. Yang and W. S. Ahn, *Chem. Eng. J.*, 2011, **168**, 1134-1139.
7. H. L. Huang, W. J. Zhang, D. H. Liu, B. Liu, G. J. Chen and C. L. Zhong, *Chem. Eng. Sci.*, 2011, **66**, 6297-6305.
8. Z. J. Zhang, S. K. Xian, H. X. Xi, H. H. Wang and Z. Li, *Chem. Eng. Sci.*, 2011, **66**, 4878-4888.
9. G. S. Xu, J. F. Yao, K. Wang, L. He, P. A. Webley, C. S. Chen and H. T. Wang, *J. Membr. Sci.*, 2011, **385**, 187-193.
10. H. Hayashi, A. P. Cote, H. Furukawa, M. O'Keeffe and O. M. Yaghi, *Nat. Mater.*, 2007, **6**, 501-506.
11. W. Morris, B. Leung, H. Furukawa, O. K. Yaghi, N. He, H. Hayashi, Y. Houndonougbo, M. Asta, B. B. Laird and O. M. Yaghi, *J. Am. Chem. Soc.*, 2010, **132**, 11006-11008.
12. D. Saha, Z. B. Bao, F. Jia and S. G. Deng, *Environ. Sci. Technol.*, 2010, **44**, 1820-1826.
13. P. L. Llewellyn, S. Bourrelly, C. Serre, Y. Filinchuk and G. Ferey, *Angew. Chem.-Int. Edit.*, 2006, **45**, 7751-7754.
14. S. Couck, J. F. M. Denayer, G. V. Baron, T. Remy, J. Gascon and F. Kapteijn, *J. Am. Chem. Soc.*, 2009, **131**, 6326-6327.
15. S. Bourrelly, P. L. Llewellyn, C. Serre, F. Millange, T. Loiseau and G. Ferey, *J. Am. Chem. Soc.*, 2005, **127**, 13519-13521.
16. P. L. Llewellyn, S. Bourrelly, C. Serre, A. Vimont, M. Daturi, L. Hamon, G. De Weireld, J. S. Chang, D. Y. Hong, Y. K. Hwang, S. H. Jhung and G. Ferey, *Langmuir*, 2008, **24**, 7245-7250.
17. L. Hamon, E. Jolimaitre and G. D. Pirngruber, *Ind. Eng. Chem. Res.*, 2010, **49**, 7497-7503.
18. P. S. Barcia, L. Bastin, E. J. Hurtado, J. A. C. Silva, A. E. Rodrigues and B. L. Chen, *Sep. Sci. Technol.*, 2008, **43**, 3494-3521.
19. B. Mu, F. Li and K. S. Walton, *Chem. Commun.*, 2009, 2493-2495.
20. S. H. Yang, J. L. Sun, A. J. Ramirez-Cuesta, S. K. Callear, W. I. F. David, D. P. Anderson, R. Newby, A. J. Blake, J. E. Parker, C. C. Tang and M. Schroder, *Nat. Chem.*, 2012, **4**, 887-894.
21. S. Biswas, J. Zhang, Z. B. Li, Y. Y. Liu, M. Grzywa, L. X. Sun, D. Volkmer and P. Van der Voort, *Dalton Trans.*, 2013, **42**, 4730-4737.